



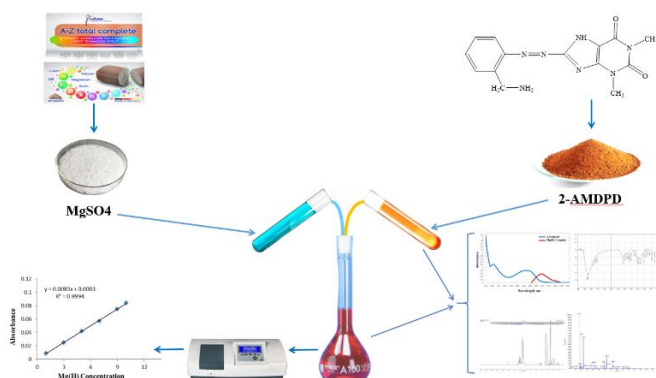
SPECTROPHOTOMETRIC DETERMINATION OF Mg(II) BY USING THEOPHYLLINE-DERIVED AZO LIGAND AS ANALYTICAL REAGENT IN PHARMACEUTICAL SUPPLEMENTS

Esraa Rasool RADHI*

Ministry of Education, Kufa, Iraq

Received June 17, 2025

One of the metals that is most abundant in cells is magnesium, due to its imperative role in cellular processes. Many diseases and pathologies in plants, animals, and humans have been related to magnesium imbalance; in contrast, the quantity of appropriate quantification techniques for the detection of magnesium is minimal. The presented study reports the synthesis of a heterocyclic azo ligand, 8-((2-(aminomethyl)phenyl)diazenyl)-1,3-dimethyl-3,7-dihydro-1H-purine-2,6-dione (2-AMDPD), formed by the combination of 2-aminobenzylamine and theophylline (1,3-dimethylxanthine) and its Mg(II) complex in excellent yields. For the Mg(II) spectrophotometric determination, the analytical reagent utilized was the synthetic azo ligand. An array of spectral techniques has been utilized to characterize the azo ligand that was synthesized and its complex with Mg(II), including UV-Vis, ¹H NMR, FT-IR, and Mass spectroscopies, in addition to the magnetic measurements and the fundamental evaluation (C.H.N). The study of molar conductivity indicates that the Mg(II) complex, being a non-electrolyte, does not exhibit the conductivity property. The obtained outcomes strengthened that the azo dye performs as a bidentate ligand, and the stoichiometric composition of the Mg(II) complex is (1:1) M:L. After optimizing the determination conditions, the Mg(II) was spectrophotometrically determined using the synthesized ligand at 518 nm. The method linearity was 1.0–10.0 μg mL⁻¹, the detection and quantitative limits were 0.417 and 1.391 μg mL⁻¹, respectively. After implementing the suggested procedure, it was possible to ascertain the Mg(II) quantity in pharmaceutical supplements with satisfactory percent recovery results in the range of 96.8–99.4%.



INTRODUCTION

When it comes to the fluid inside cells, magnesium is second in abundance, and it ranks fourth overall in the human body. Still, there is a lack of information about the analytical and clinical

importance, as well as the consequent impact of the imbalance of measurable magnesium. The divalent magnesium ion is the primary intracellular cation and exhibits unique characteristics based on its chemical structure. Unlike the other cations, the magnesium hydration shell cannot be easily

* Corresponding author: esraar.falfali@student.uokufa.edu.iq

stripped, greatly extending its radius and influencing its biological behavior through steric constraints.¹ The soil, fertilizers, irrigation water, and cooking and processing methods all have a significant impact on the magnesium content of food. Legumes, seeds, nuts, whole grain bread, cereals, cocoa, and some fruits constitute excellent magnesium sources.²

Although the hormonal regulation of calcium ions is mediated by the parathyroid gland, the hormonal regulation of magnesium ions, despite its important role in human health, is minimal. Therefore, the latter ion has been called the forgotten or orphan ion.³ Numerous conventional analytical methods are being applied to measure the Mg(II) quantity in fixed or live samples with variable confidence levels; such as atomic absorption spectrometer,⁴⁻⁶ ³¹P-MRS which symbolizes phosphorus magnetic resonance spectroscopy,⁷⁻⁹ proton NMR,¹⁰ clinical NMR instruments,¹¹ ICP-AES which symbolizes inductively coupled plasma-atomic emission spectrometry,^{12,13} Ion Selective Electrodes,¹⁴ Optical chemosensors,¹⁵ Fluorescent Chemosensors,¹⁶⁻¹⁸ analytical scanning electron microscopy (ASEM).^{19,20} These methods have assigned benefits and drawbacks; the phosphorus magnetic resonance spectroscopy method demanded cumbersome sample pretreatment, complicated instruments, and a long time, in addition to not being able to derive information about the intracellular magnesium distribution by this method. The ICP-AES method is considered a destructive technique that requires specialized staff to implement and does not allow differentiation between the bound and free forms of the analyzed ion. The main disadvantages of the ion-selective electrodes are the lack of electrode specificity, the relatively long reaction times, and the effect of several interferences, like changes in pH, on the ion complex in the specified samples.

A group of organic compounds called azo compounds emerges because of the many ways they can be used in pharmaceuticals, food coloring, textile dyeing, and cosmetics.²¹⁻²³ Furthermore, Azo ligands having heterocyclic moieties have made notable advances in electronics, such as optoelectronic devices, and storage;²⁴ as compared with simple aromatic chemical compounds,²⁵ heterocyclic azo compounds have a dramatic batho effect.²⁶ These compounds are unique because of their functional groups (-N=N-), which act as an efficient analytical chromophore and give magnificent coloring characteristics to the

synthesized azo compounds bound to the aromatic and/or heterocyclic systems.²⁷

The presence of heterocyclic compounds containing nitrogen, sulfur, or oxygen in the azo ligand molecules enhances the color of these compounds, makes them more stable, and improves their solvatochromic behaviour.^{28,29} In addition, azo compounds derived from heterocyclic compounds demonstrated notable anticancer, antioxidant, antiviral, insecticide, antibacterial, antidiabetic, and other chemotherapeutic properties.^{30,31} Both natural and synthetic azo compounds are regarded as beginning points for pharmaceutical discovery and are a major source of drug prototypes.³² For this investigation, a quick, sensitive, and simple spectrophotometric procedure for the Mg(II) determination using an azo ligand derived from theophylline as an analytical reagent was implemented. The complex of Mg(II) with the azo ligand that were synthesized were defined by an array of spectral techniques, including Mass spectroscopy, UV-Vis, FT-IR, and ¹H NMR. In addition, the molar conductivity study, magnetic observations, and elemental analysis (C.H.N.) were carried out. Mg(II) in pharmaceutical supplements was successfully determined using the suggested method, yielding satisfactory recovery outcomes.

MATERIALS AND METHODS

Materials and instruments

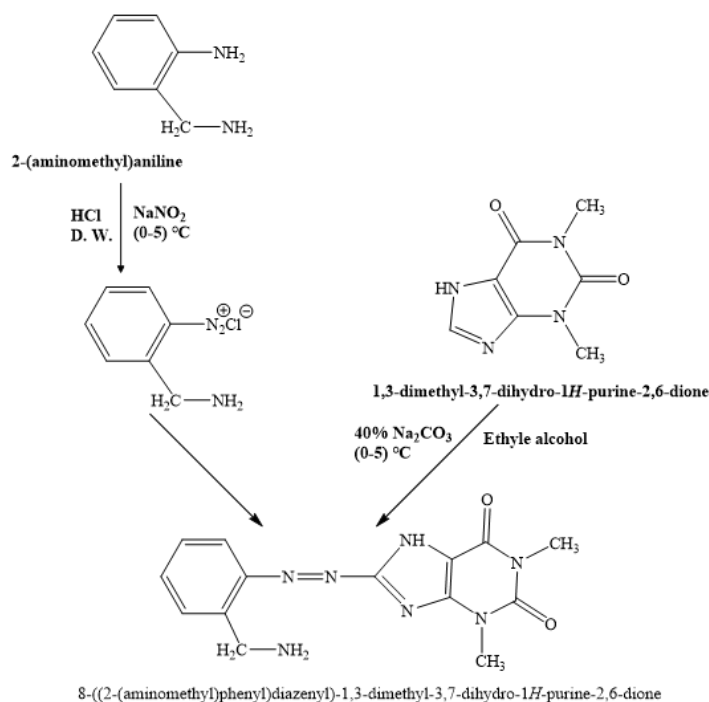
In the current study, every chemical and solvent employed for the synthesis and characterization is of analytical reagent grade. A Shimadzu (UV-1700) double-beam spectrophotometer with glass cells (1 cm) served to obtain the UV-VIS spectra, and a Shimadzu spectrophotometer with a KBr disks were employed for identifying the FT-IR spectra. The mass spectrum was conducted employing the Shimadzu Agilent HP (5973) mass spectrometer, and ¹H-NMR spectra were acquired utilizing a Bruker Biospin Gmph 500 MHz spectrophotometer in dimethyl sulfoxide-d₆ solvent and tetramethylsilane (the internal standard). The Mg(II) determination in the pharmaceutical supplements was utilizing the Shimadzu AA-6800 atomic absorption spectrometer combined with a graphite furnace atomizer, and utilizing dimethyl sulfoxide as a solvent, molar conductivity values were determined utilizing the digital conductivity series ion. lab. 720 instruments. While in order to find the compounds' melting points, the Stuart-

SMP10 point of melting apparatus was utilized. To measure the pH values, the Oakton 2100 pH Meter was employed; the pH values were measured by the Oakton 2100 pH Meter.

Preparation of 8-((2-(aminomethyl)phenyl)diazenyl)-1,3-dimethyl-3,7-dihydro-1H-purine-2,6-dione Ligand

In 30 mL of distilled water at a temperature of 0–5 °C, 1.222 g (0.01 mol) of 2-aminobenzylamine was thawed to produce the Azo Ligand, after which, while stirring slightly, while keeping the solution at the indicated temperature, add 5 mL of concentrated HCl acid. Sodium nitrite solution, made by addition 0.700 g of sodium nitrite (0.01 mol) to 10 mL of distilled water and stirring until dissolved, while

keeping the temperature between 0 and 5 °C, with constant stirring, was added gradually (drop by drop). To collect the diazonium solution, the resulting solution was given time to set for an hour. Subsequently, the diazonium solution was poured into the coupling component solution, made by addition 1.802 g (0.01 mol) of theophylline (1,3-dimethylxanthine) in 20 mL of 40% Na₂CO₃ solution. Then, while keeping the temperature between 0 and 5° C and the acidity of the solution at a pH of approximately 7, 50 mL of ethanol was used while being stirred. For a day, the final solution was left to set; the formed azo crystals were then filtered, rinsed employing distilled water, re-crystallized in absolute ethanol, and finally dried in the air. The 2-AMDPD preparation procedure is demonstrated in Scheme 1.



Scheme 1 – The 2-AMDPD azo ligand preparation procedure.

Preparation of the 2-AMDPD-Mg(II) complex

In order to create the Mg(II) complex with the ligand 8-((2-(aminomethyl)phenyl)diazenyl)-1,3-dimethyl-3,7-dihydro-1H-purine-2,6-dione, a solution of (0.246 g, 0.001 mol) MgSO₄·7H₂O dissolved in 5 mL DMSO was mixed, 1 mL of NaOH solution with a concentration of 0.1 M, and the solution of (0.001 mol, 0.313 g) 2-AMDPD azo ligand mixed with 20 mL DMSO to get a molar ratio of 1:1 [M:L]. After letting the solution set and precipitate for 24 hours, the formed complex

crystals were filtered, dried. Then the resulting complex recrystallization was performed in absolute ethanol.

The standard and work solutions' preparation

A flask with a volume of 100 mL was used to create a 100 µg mL⁻¹ Mg(II) ion stock solution by pouring 0.101 g of magnesium sulphate heptahydrate MgSO₄·7H₂O in enough distilled water and then adding the remaining solvent to fill the flask. The dilution method was followed with

the same solvent to prepare the Mg(II) diluted working solutions. To prepare the 1×10^{-2} mol L⁻¹ 2-AMDPD azo ligand stock solution in a flask with a volume of 100 mL, 0.313 g azo ligand was poured in a sufficient dimethyl sulfoxide solvent followed by completion the flask volume utilizing the same solvent. The dilution method was followed to prepare the ligand working solutions in the same solvent.

A solution of the specific interference cations with 100 µg mL⁻¹ was formulated in a flask with a volume of 100 mL *via* liquefying suitable amounts of the different cations' chloride salts with sufficient distilled water, and finalizing the volume of the flask consuming the same solvent. The stock solutions with 100 µg mL⁻¹ of the specific interference anions in a 100 mL volumetric flask were formulated by combining amounts of the different anions' sodium salts with distilled water, followed by completion the flask volume utilizing the same solvent. The different interference ions working solutions were arranged utilizing the same solvent, following the dilution method. To prepare a stock solution with 100 µg mL⁻¹ of the specified pharmaceuticals, 10 tablets or capsules of each pharmaceutical were ground and well mixed, and an accurate weighted amount of each pharmaceutical containing 0.01 g Mg(II) was dissolved in sufficient distilled water. The solution was passed through a Whatman No. 1 filter before being transferred to a volumetric flask of 100 mL. To fill up the remaining volume, distilled water was added.

General determination procedure

Consuming a sequence of 10 mL volumetric flasks, suitable volumes of Mg(II) stock solution holding 1–10 µg mL⁻¹ were poured, followed by addition 0.1 mL of 5×10^{-3} mol L⁻¹ 2-AMDPD

solution and 0.1 mL of NaOH solution (0.1 M). Finally, every flask was filled with distilled water to make it the proper volume for diluting the solution. The solution absorbance was determined after 3 minutes against the blank absorbance at 518 nm. Subsequently, a curve for calibration was plotted using the complex absorbance values and Mg(II) concentration values.

RESULTS AND DISCUSSION

Characterization of 2-AMDPD ligand and its Mg(II) complex

The crystalline form is achieved by obtaining the azo ligand and its Mg(II) complex, which are 8-((2-(aminomethyl)phenyl)diazonyl)-1,3-dimethyl-3,7-dihydro-1H-purine-2,6-dione, and they exhibit, at room temperature, high stability to air and humidity. The azo ligand possesses an orange color, while its complex with Mg(II) is red. The two prepared compounds are to be insoluble in water, ethanol, and methanol; and freely soluble in chloroform, acetone, dimethyl sulfoxide, and dimethylformamide. The magnetic susceptibility value measured for the complex confirmed the tetrahedral geometry (Sp³), and the molar conductivity data obtained pointed to the non-electrolytic nature of this complex. The C.H.N elemental analysis outcomes of the Mg complex are in line with those calculated for the complex suggested formula and correspond with a 1:1 (ligand: metal) stoichiometry ratio. The 2-AMDPD azo ligand and its Mg(II) complex were categorized utilizing UV–Vis spectrophotometry, ¹H-NMR, FT-IR, mass spectral analysis, and C.H.N elemental analysis. Table 1 shows the physical and analytical characteristics of the prepared compounds.

Table 1

The Analytical and Physical properties of 2-AMDPD and its Mg(II) complex

Compound	Color Yield %	M. p. °C	M. f M. wt	*Found % (Calc.) %					
				C	H	N	O	S	M
Ligand C ₁₄ H ₁₅ N ₇ O ₂	Orange	132–134	313.31	53.58 (53.62)	4.72 (4.78)	31.22 (31.27)	10.18 (10.21)	----	----
[Mg (L)SO ₄]	Red	198–200	433.69	38.70 (38.73)	3.39 (3.45)	22.57 (22.59)	22.10 (22.13)	7.31 (7.37)	5.56 5.60

*Found % = the experimental values, Calc. % = the calculated values

Electronic spectra of 2-AMDPD ligand and the Mg(II) complex

Figure 1 displays the recorded electronic spectra of the 2-AMDPD azo ligand and its Mg(II) complex. The electronic transitions $n \rightarrow \pi^*$ and $\pi \rightarrow \pi^*$ were identified as the sources of the two absorption peaks in the azo ligand spectrum, which were detected at 445 and 285 nm, respectively.^{33,34}

In the Mg(II) complex spectrum, the peak of the electronic transition $n \rightarrow \pi^*$ is subject to a bathochromic shift to a higher wavelength, 518 nm, indicating the coordination with the Mg(II) to form a stable complex, the non-electrolyte Mg(II) complex has a tetrahedral geometry Sp^3 . Table 2 lists the two prepared compounds' electronic spectral data. Scheme 2 shows the proposed complex structure.

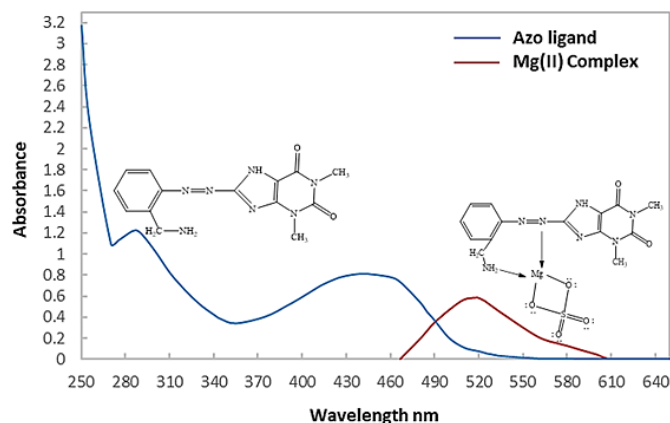
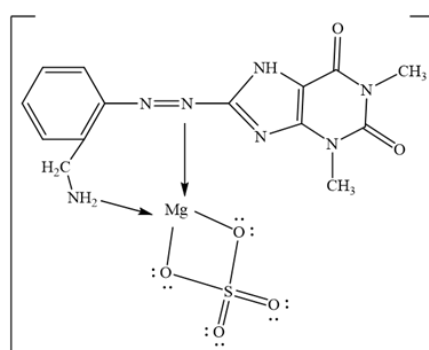


Fig. 1 – Electronic spectra of the synthesized azo ligand and its Mg(II) complex.

Table 2

Electronic transitions, magnetic moment, the proposed geometry, and hybridization of the Mg(II) complex

Compounds	λ_{\max} nm	Absorption bands cm^{-1}	Transition	A_m $\Omega^{-1} \cdot \text{mol}^{-1} \cdot \text{cm}^2$	μ_{eff} B.M	Geometry	Hybridization
Ligand =L ($\text{C}_{14}\text{H}_{15}\text{N}_7\text{O}_2$)	285	35087	$\pi \rightarrow \pi^*$	----	----	----	----
[Mg(L)SO ₄]	518	19305	$n \rightarrow \pi^*$	0.5	----	tetrahedral	Sp^3



Scheme 2 – The proposed structure of the 2-AMDPD complex with Mg(II).

Infrared spectra of 2-AMDPD ligand and the Mg(II) complex

FT-IR spectra of the synthesized azo ligand and its Mg(II) complex were obtained as presented in Fig. 2. The free azo ligand displayed a sharp and strong stretching vibration at 1600 cm^{-1} , returning

to the (C=N) group in the 1,3-dimethylxanthine molecule.³⁵ This vibration remains at the same frequency in the Mg(II) complex spectrum, confirming that none of these individuals were involved in the process of coordinating with the Mg(II) ion. The free azo ligand also displayed sharp and strong vibrations at 1435 and 1460 cm^{-1} ,

corresponding to the azo group with (N=N) in the molecule;³³ these bands' absorption was shifted to lower frequencies at 1400 and 1433 cm^{-1} in the Mg(II) complex spectrum. In the ligand spectrum, two stretching bands at 3360 and 3429 cm^{-1} are observed owing to the NH_2 group,^{36,37} these bands are detected (3394 and 3439 cm^{-1}) in the spectrum

of the Mg complex, this shifting in the bands' vibration indicates the participation of the azo (N=N) and amine (N-H) groups in the complex formation. The complex spectrum displays a band at 428 cm^{-1} , that is ascribed to the (Mg-N) bond. You can find the infrared data of 2-AMDPD and the Mg(II) complex in Table 3.

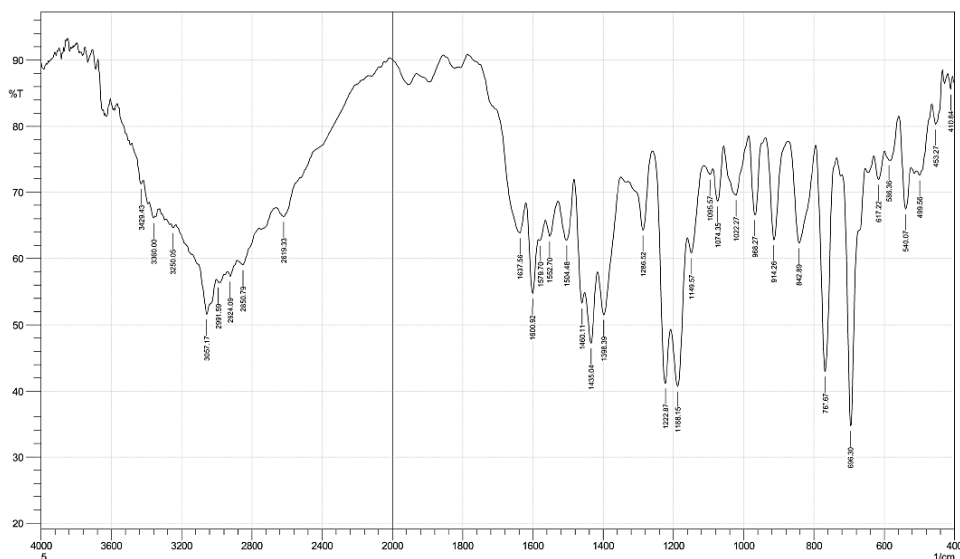


Fig. 2– FT-IR spectra of 2-AMDPD.

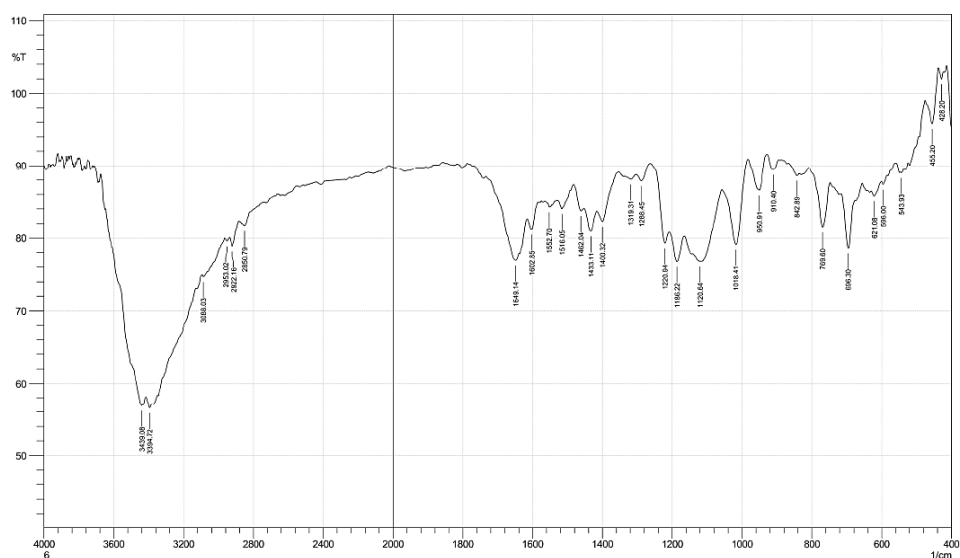


Fig. 3– FT-IR spectra of 2-AMDPD complex with Mg(II).

Table 3

Selected IR absorption bands for the two prepared compounds in cm^{-1}

Compound	ν (N-H)	ν (C-H)	ν (C=O)	ν (C-H)	ν (C=N)	ν (C=C)	ν (N=N)	ν (M-N)
		Ar.		Aliph.	Endo.	Ar.		
Ligand =L ($\text{C}_{14}\text{H}_{15}\text{N}_7\text{O}_2$)	3360 w. 3429 w.	3057 m.	1637 w.	2850 w.	1600 m.	1552 w.	1435 m. 1460 m.	----
[Mg(L)SO ₄]	3394 s. 3439 s.	3088 w.	1649 w.	2850 w.	1602 w.	1552 w.	1400 w. 1433 w.	428 w.

s. = strong m.= medium, w.= weak, Ar.= aromatic, Aliph.= Aliphatic, Endo. = endo bond

¹H NMR spectra of 2-AMDPD azo ligand and the Mg(II) complex

The azo ligand and its Mg(II) complex ¹H NMR spectra are shown in Fig. 3. The azo spectrum showed multiple signals at 6.81–6.99 ppm attributed to the NH₂ protons, while it appears as a weak multiple signal in the same position in the Mg(II) complex spectrum. The multiple signals observed at 7.02–7.88 ppm in the ligand spectrum³⁶ and at 7.40–7.88 ppm in the Mg(II) complex

spectrum are recognized as the result of the aromatic ring protons and heterocyclic ring protons. The NH₂ group exhibits a signal at 7.93 and 7.94 ppm in the organized ligand and its complex with Mg(II), respectively.³⁶ The N-H protons in the imidazole ring show a signal at 9.8 and 10.1 ppm in the ligand and the Mg(II) complex spectra, respectively. In both spectra, there is a signal at 3.4 ppm assigned to the methyl group in the theophylline.^{33,34} The protons in the DMSO solvent were attributed the signal that appeared at $\delta = 2.52$ in both spectra.

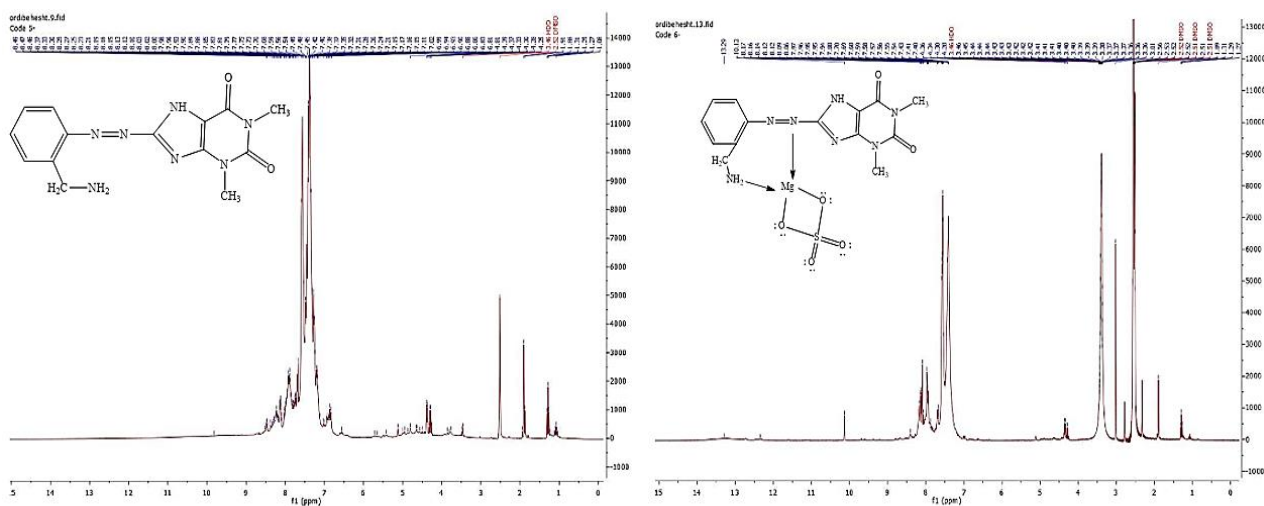


Fig. 4 – ¹H NMR spectra of the 2-AMDPD azo ligand and its Mg(II) complex.

Mass spectra of 2-AMDPD ligand and the Mg(II) Complex

Mass spectrometry characterized the azo ligand and its Mg(II) complex; the mass spectrum results confirmed the molecular weight of the two compounds and were consistent with the calculated values. As shown in Fig. 4, it's apparent that the azo

ligand's molecular ion peak is at $m/z^+ = 315$, corresponding to the $[C_{14}H_{15}N_7O_2]^+ + 2H^+$ species. The Mg(II) complex's molecular ion peak at $m/z^+ = 433$ does not appear because of the large molecular weight, the presence of many heterogeneous atoms in the complex structure, and the high bombardment energy.³⁸ Table 4 highlights the proposed fragments of the two compounds throughout decomposition.

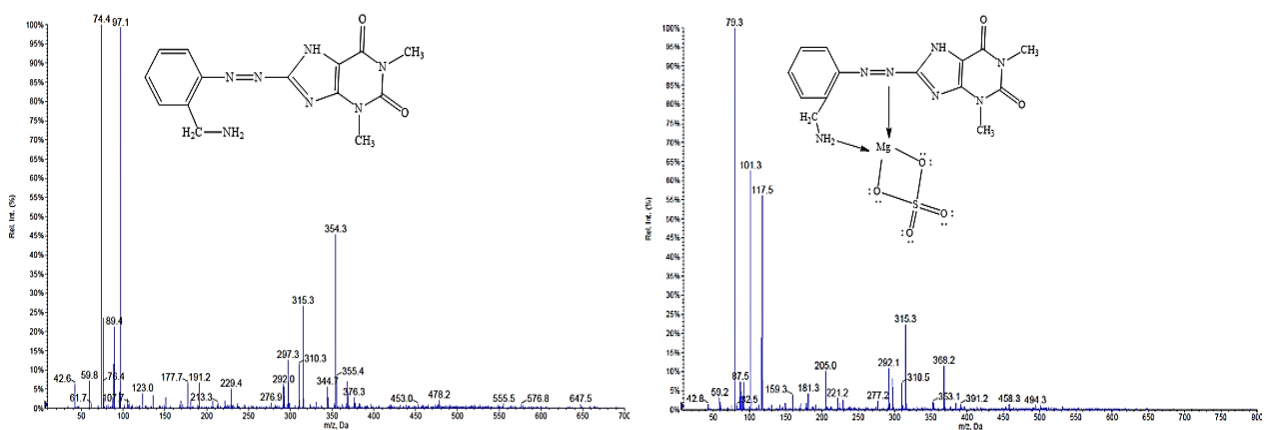


Fig. 5 – Mass spectra of the 2-AMDPD ligand and its Mg(II) complex.

Table 4

The Mass Spectra data of the 2-AMDPD ligand and its Mg(II) complex

2-AMDPD ligand		2-AMDPD -Mg(II) complex	
The proposed Fragment	m/z^+ (Base peak %)	The proposed Fragment	m/z^+ (Base peak %)
[C ₁₄ H ₁₅ N ₇ O ₂]+2H ⁺	315 (27 %)	[C ₁₃ H ₁₅ N ₇ O ₆ SMg]	421 (1 %)
[C ₁₄ H ₁₅ N ₇ O ₂]	313 (3 %)	[C ₁₂ H ₁₁ N ₆ O ₆ SMg]	391 (2%)
[C ₁₄ H ₁₂ N ₇ O ₂] ⁺	310 (12 %)	[C ₁₁ H ₉ N ₆ O ₅ SMg]	361(1%)
[C ₁₄ H ₁₃ N ₆ O ₂] ⁺	297 (13 %)	[C ₁₁ H ₁₅ N ₅ O ₅ SMg] ⁺	353 (3%)
[C ₁₃ H ₁₀ N ₆ O ₂] ⁺	282 (2 %)	[C ₁₀ H ₈ N ₅ O ₄ SMg] ⁺	318 (1%)
[C ₁₂ H ₈ N ₆ O ₂] ⁺	268 (1%)	[C ₁₄ H ₁₅ N ₇ O ₂]+2H ⁺	315 (24 %)
[C ₁₁ H ₉ N ₄ O ₂] ⁺	229 (5%)	[C ₁₀ H ₁₁ N ₅ Mg]	225 (2%)
[C ₁₀ H ₉ N ₆] ⁺	213 (3%)	[C ₇ H ₅ N ₆ O ₂] ⁺⁺	205 (11%)
[C ₇ H ₇ N ₆ O ₂] ⁺	207 (2%)	[C ₇ H ₉ N ₄ O ₂] ⁺	181 (4%)
[C ₇ H ₇ N ₃] ⁺	133 (1%)	[C ₅ H ₁₁ N ₄ O ₂] ⁺	159 (4%)
[C ₇ H ₁₁ N ₂] ⁺	123 (4%)	[C ₅ H ₁₁ N ₃ O ₂]	145 (1%)
[C ₃ H ₅ N ₄] ⁺	97 (99%)	[C ₄ H ₉ N ₂ O ₂]	117 (56%)
[C ₆ H ₄] ⁺⁺	76 (24%)	[C ₄ H ₉ N ₂ O] [*]	101 (63%)
[C ₄ H ₁₁] ⁺	59 (7%)	[C ₄ H ₆ N ₂]	82 (2%)

Optimization of analytical conditions of the spectrophotometric determination of Mg(II) by the prepared azo ligand

All the analytical conditions that could affect the suggested determination method for Mg(II) have been studied and optimized by changing each condition independently while keeping the others constant.

Azo ligand concentration effect

Utilizing 2.0 mL of an aqueous solution containing 0.1 mL of azo ligand solution, 7.0 $\mu\text{g mL}^{-1}$ of Mg(II), and a 0.1 mL NaOH solution with a concentration of 0.1 M, the range of 1×10^{-3} to 1×10^{-2} mol L⁻¹ was utilized to calculate the effect of azo ligand concentration on the complexation reaction. When comparing the absorbance of the blank with that of the final solution at 518 nm, the absorbance of the azo ligand solution with a concentration of 5×10^{-3} mol L⁻¹ had the highest value (Fig. 5A).

Azo ligand solution volume effect

The azo ligand solution volume effect on the Mg(II) complex construction was determined using 2.0 mL of Mg(II) aqueous solution with a concentration of 7.0 $\mu\text{g mL}^{-1}$, a 0.1 mL NaOH solution with a concentration of 0.1 M, and azo ligand solution with a concentration of

5×10^{-3} mol L⁻¹ in the range of 0.05–0.30 mL. The final solution absorbance was measured by comparing the absorbance of a blank with azo ligand solutions of varying volumes measured at 518 nm. Using 0.10 mL of the ligand resulted in the highest absorbance (Fig. 5B).

Time and temperature effect

The establishment and stability of the Mg(II) complex as a function of reaction time and temperature were considered between 1.0 and 30.0 minutes for the reaction time and 25–50 °C for the reaction temperature. The outcomes exhibit that the absorbance of the complex rises with the time of reaction up to 3 minutes, and the complex remains stable for around 8 hours. This stability was noticed at room temperature till 40 °C, and then the decrease in the absorbance value was registered at higher temperatures.

Mg(II) solution volume effect

Incorporating 0.1 mL of 0.1 M NaOH solution, 0.1 mL of 5×10^{-3} mol L⁻¹ azo ligand, and 7.0 $\mu\text{g mL}^{-1}$ Mg(II) solution, the Mg(II) solution volume effect was checked in the range of 1.0–3.0 mL. Measuring the absorbance value of the final solution at various volumes of Mg(II) solution at 518 nm versus the absorbance of the blank revealed

that, using 2.0 mL of Mg(II) solution, the maximum absorbance was achieved (Fig. 5C).

Sodium hydroxide solution concentration effect

A measurement was taken of the effect of NaOH concentration on complex formation using 0.1 mL

NaOH solution, 0.1 mL of azo ligand with $5 \times 10^{-3} \text{ mol L}^{-1}$ concentration, and 2 mL, $7.0 \mu\text{g mL}^{-1}$ of Mg(II) solution. Measuring the absorbance value of the final solution in the range of 0.05–0.50 M NaOH solution concentrations against the absorbance of the blank demonstrated that the maximum absorbance was reached using 0.10 M of NaOH (Fig. 5D).

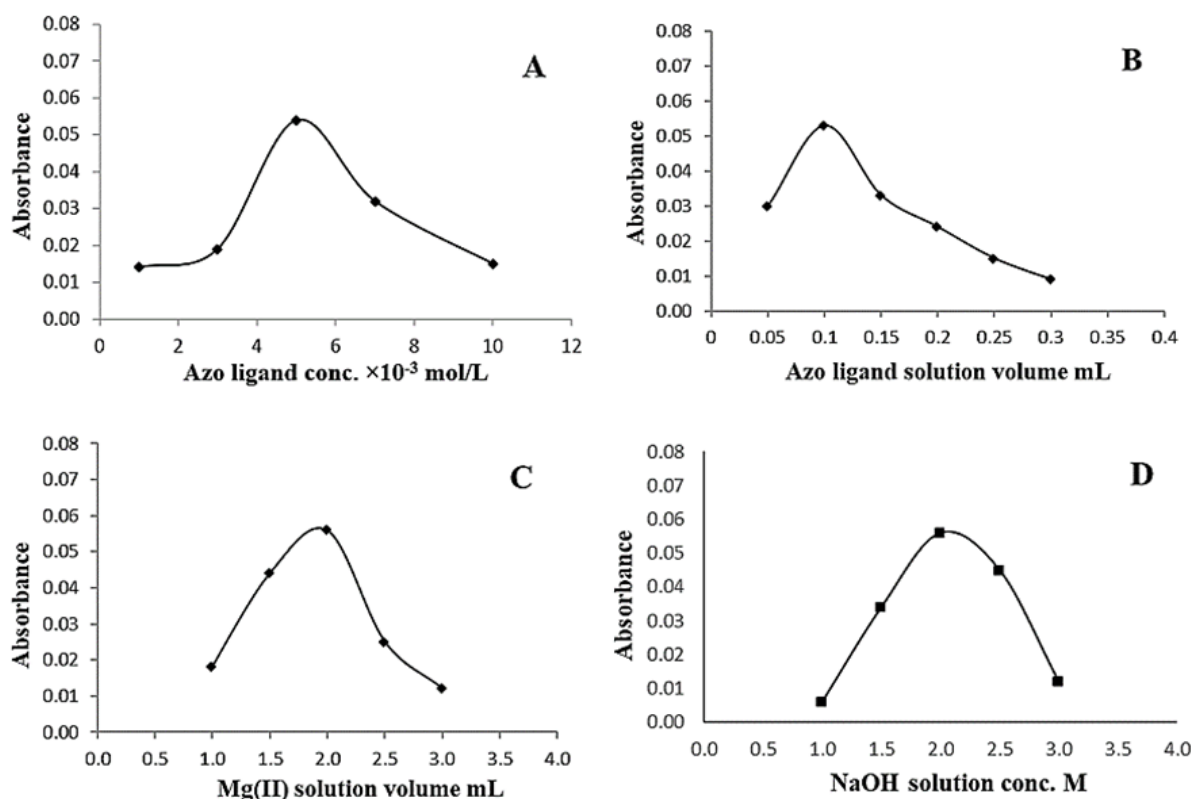


Fig. 6 – The outcome of various analytical conditions on the Mg(II) spectrophotometric determination.

Sodium hydroxide solution volume effect

The effect of NaOH solution volume on the complexation reaction was tested using 0.1 mL of azo ligand with $5 \times 10^{-3} \text{ mol L}^{-1}$, 0.1 M NaOH solution, and 2 mL, $7.0 \mu\text{g mL}^{-1}$ of Mg(II) solution. Absorbance at 518 nm was measured for complex solutions with volumes that varied from 0.05 to 0.50 mL of NaOH, and According to the results, 0.10 mL of NaOH was the optimal concentration for achieving maximum absorbance.

Evaluation of the suggested determination method

According to the mentioned experiments, in order to obtain the calibration curve, five replicates

of various Mg(II) aqueous solutions with varying concentrations were prepared, then drawing the calibration relationship between the measured absorbance values for these solutions, that measured against the blank absorbance at 518 nm, and the specified concentration values. The suggested method linearity was in the range of concentrations from 1.0 to $10.0 \mu\text{g mL}^{-1}$ of Mg(II). To evaluate the determination method's sensitivity, two limits of quantitation and detection were determined. The reliability of the procedure was assessed by calculating the RSD% of ten independent samples that contain $7.0 \mu\text{g mL}^{-1}$ of Mg(II) using the proposed method. The RSD% value equaled 0.876, pointing to the proposed method's high level of precision. Table 5 shows the obtained analytical data.

Table 5

The obtained analytical data of the Mg(II) determination method

Analytical parameter	Data
λ_{max} nm	518
Regression equation	$y = 0.0083x + 0.0003$
Specific absorption coefficient ($\text{L gm}^{-1} \text{cm}^{-1}$)	8.3
Molar absorption coefficient ($\text{L mol}^{-1} \text{cm}^{-1}$)	$0.202 \times 10^{+3}$
Sandells sensitivity ($\mu\text{g cm}^{-2}$)	1.205×10^{-4}
Correlation coefficient r^2	0.9994
Detection limit ($\mu\text{g mL}^{-1}$)	0.417
Quantitation limit ($\mu\text{g mL}^{-1}$)	1.391
Linear range ($\mu\text{g mL}^{-1}$)	1.0 – 10.0
Standard deviation (n =10)	0.001
Relative standard deviation % (n =10)	0.876

The Interference Effect Study

The interfering outcome of certain anions and cations that might be competing with the Mg(II) or with the azo ligand in the Mg(II) complex construction or affecting its steadiness was studied to examine the selectivity of the proposed method. By implementing the general determination procedure with $7.0 \mu\text{g mL}^{-1}$ Mg(II) synthetic solutions comprising the tested interfering ions in two amounts of 1:1 and 1:10 (w/w) ion:interference. Different masking agents were studied to eliminate the tested cations' interfering

effect, such as NaOH, NH_3 , citric acid $\text{C}_6\text{H}_8\text{O}_7$, and $\text{NaH}_2\text{PO}_4 \cdot 2\text{H}_2\text{O}$.

As shown in Table 6, the citric acid solution was an active masking agent (with different concentrations and volumes) for Mn(II) and Ca(II) interference. While NaOH was used for masking Zn(II) and NaH_2PO_4 was used for masking Fe(III) interference, with no interfering effect of Cu(II) on the complex development. Also, at the two levels of interference that were considered, the formation and stability of the Mg(II) complex were unaffected by numerous anions, including NO_3^- , SO_4^{2-} , Cl^- , CrO_4^{2-} , and $\text{CH}_3\text{COO}^{2-}$.

Table 6

The interference effect on Mg(II) determination and the appropriate masking agent concentration and volume

Interference type	*Interference conc. ($\mu\text{g mL}^{-1}$)	Masking agent conc. (M)	Masking volume (mL)	agent	Recovery%
Zn(II)	7	0.50 NaOH	0.2		99.1
	70	0.50 NaOH	0.2		98.8
Mn(II)	7	0.10 $\text{C}_6\text{H}_8\text{O}_7$	0.1		97.7
	70	0.10 $\text{C}_6\text{H}_8\text{O}_7$	0.1		98.6
Cu(II)	7	–	–		99.8
	70	–	–		99.8
Fe(III)	7	0.05 NaH_2PO_4	0.1		97.7
	70	0.05 NaH_2PO_4	0.8		98.4
Ca(II)	7	0.012 $\text{C}_6\text{H}_8\text{O}_7$	0.1		97.7
	70	0.012 $\text{C}_6\text{H}_8\text{O}_7$	0.2		96.9

*The Mg(II) concentration is $7 \mu\text{g mL}^{-1}$

The Applications

The accuracy of the suggested Mg(II) determination method, denoted as the percentage

recovery determination, utilizing the azo ligand that was synthesized as an analytical tool, was investigated by replicating the spectral measurements of $7 \mu\text{g mL}^{-1}$ Mg(II) containing

pharmaceutical supplement solutions (n = 5). As shown in Table 7, the recovery percentage fell between 96.8% and 99.4%. To confirm the applicability and viability of the submitted method, these results were compared with flame atomic absorption spectrometry technique results as a

reference determination method, the results were in good conformance with them. This agreement indicates that the presented method could be applied for Mg(II) determination in varying pharmaceutical formulations with high accuracy, precision, and sensitivity.

Table 7

The Mg(II) determination by the suggested method in pharmaceuticals

Sample	Taken value	by the suggested method			by FAAS method		
		found value	*E %	Rec. %	found value	*E %	Rec. %
A-Z total complete (100 mg / tablet)	7	6.873	-1.814	98.2	6.982	-0.257	99.7
Sentry (100 mg / tablet)	7	6.869	-1.871	98.1	6.883	-1.671	98.3
MAGESIUM GLYCINATE (400 mg / capsule)	7	6.776	-3.191	96.8	6.785	-3.071	96.9
CAL-D-VIT (450 mg / tablet)	7	6.794	-2.943	97.1	6.872	-1.829	98.2
Triple Magnesium Complex (400 mg / capsule)	7	6.807	-2.758	97.2	6.990	-0.142	99.8
Candida Support (45 mg / capsule)	7	6.96	-0.572	99.4	7.112	1.6	101.6

*Percent error for tested samples (n = 5)

CONCLUSION

The synthesized azo ligand formed by the combination of 2-amino benzylamine and theophylline and its Mg(II) complex were prepared and subjected to structural characterization applying C.H.N element content analysis, mass spectroscopy, ¹H-NMR, UV-Vis, and FT-IR, besides the magnetic susceptibility measurements. The spectroscopic analysis indicated that the Mg(II) complex stoichiometric ratio is 1:1 (M:L) with an octahedral geometry. In order to achieve a rapid, efficient, and straightforward spectroscopic measurement of the magnesium ion, the azo that was synthesized was successfully utilized as an analytical reagent. This was accomplished by forming a stable reddish-orange complex at 518 nm. The linearity of the azo fell between 1.0 and 10.0 µg mL⁻¹ to achieve the desired results. The interfering outcome of certain anions and cations that could exist in pharmaceutical supplements was checked, and appropriate masking agents were chosen to eliminate the interfering ions' influence. The suggested approach was additionally utilized for the measurement of Mg(II) in diverse pharmaceutical supplements with promising recovery results.

REFERENCES

1. A. Dent and R. Selvaratnam, *Clin. Biochem.*, **2022**, *105*, 1–15.
2. A.M. Romani, *Arch. Biochem. Biophys.*, **2011**, *512*, 1–23.
3. S.T. Reddy, S.S. Soman and J. Yee, *Advances in chronic kidney disease*, **2018**, *25*, 224–229.
4. A. Arif, B. Khan, K. Majeed, M.S. Shahzad, M.S. Nadeem and R. Ahmed, *South Asian Journal of Life Sciences*, **2018**, *6*, 14–21.
5. G. Lutfullah, A.A. Khan, A.Y. Amjad and S. Perveen, *The scientific world journal*, **2014**, *2014*, 715845.
6. R. Rehman and T. Tanveer, *Bulg. Chem. Commun.*, **2019**, *51*, 206–211.
7. D. Cameron, A.A. Welch, F. Adelnia, C.M. Bergeron, D.A. Reiter, L.J. Dominguez, N.A. Brennan, K.W. Fishbein, R.G. Spencer and L. Ferrucci, *Frontiers in Physiology*, **2019**, *10*, 1454.
8. M. Nelander, J. Weis, L. Bergman, A. Larsson, A.K. Wikström and J. Wikström, *Am. J. Hypertens.*, **2017**, *30*, 667–672.
9. N.W. Lutz and M. Bernard, *J. Magn. Reson.*, **2018**, *294*, 71–82.
10. H. Reyngoudt, A.L. Lopez Kolkovsky and P.G. Carlier, *NMR Biomed.*, **2019**, *32*, e4115.
11. J.C. Schutten, A.W. Gomes-Neto, G. Navis, R.T. Gansevoort, R.P. Dullaart, J.E. Kootstra-Ros, R.M. Danel, F. Goorman, R.O. Gans, M.H. de Borst and E.J. Jeyarajah, *J. Clin. Med.*, **2019**, *8*, 169.
12. K. Schilling, F. Larner, A. Saad, R. Roberts, H.M. Kocher, O. Blyuss, A.N. Halliday and T. Crnogorac-Jurcevic, *Metallomics*, **2020**, *12*, 752–757.

13. J. Ma, L. Yan, T. Guo, S. Yang, Y. Liu, Q. Xie, D. Ni and J. Wang, *Sci. Rep.*, **2020**, *10*, 10875.
14. C.Y. Fu, S.J. Chen, N.H. Cai, Z.H. Liu, M. Zhang, P.C. Wang and J.N. Zhao, *Neurol. Res.*, **2019**, *41*, 378–383.
15. L. Lvova, C.G. Gonçalves, C. Di Natale, A. Legin, D. Kirsanov and R. Paolesse, *Talanta*, **2018**, *179*, 430–441.
16. M. Liu, X. Yu, M. Li, N. Liao, A. Bi, Y. Jiang, S. Liu, Z. Gong and W. Zeng, *RSC Adv.*, **2018**, *8*, 12573–12587.
17. N. Yadav, R. Kumar, A.K. Singh, S. Mohiyuddin and P. Gopinath, *Spectrochim. Acta, Part A*, **2020**, *235*, 118290.
18. Q. Lin and D. Buccella, *J. Mater. Chem. B*, **2018**, *6*, 7247–7256.
19. N. Zghoul, N. Alam-Eldin, I.T. Mak, B. Silver and W.B. Weglicki, *Diabetes, Metab. Syndr. Obes.: Targets Ther.*, **2018**, *11*, 389–400.
20. G. Picone, C. Cappadone, A. Pasini, J. Lovecchio, M. Cortesi, G. Farruggia, M. Lombardo, A. Gianoncelli, L. Mancini, M. Ralf H and S. Donato, *Int. J. Mol. Sci.*, **2020**, *21*, 2368.
21. A.S. Waheeb, *J. Mol. Struct.*, **2023**, *1276*, 134729.
22. S. Benkhaya, S. M'rabet and A. El Harfi, *Heliyon*, **2020**, *6*, e03271.
23. K.J. Al-Adilee and M.A. Abood, *Results Chem.*, **2023**, *6*, 101145.
24. R. Hagen and T. Bieringer, *Adv. Mater.*, **2001**, *13*, 1805–1810.
25. N.M. Mallikarjuna and J. Keshavayya, *Journal of King Saud University-Science*, **2020**, *32*, 251–259.
26. S.A. Diwan and A.F. Hussain, *International Journal of Health Sciences*, **2023**, *6*, 4754–4773.
27. D. muhammed Aziz, S.A. Hassan, D.M. Mamand and K. Qurbani, *J. Mol. Struct.*, **2023**, *1284*, 135451.
28. D.B. Vishani and A. Shrivastav, *Development in Wastewater treatment research and processes*, **2022**, 419–432.
29. H.A.K. Kyhoiesh K.J. and Al-Adilee, *Results Chem.*, **2021**, *3*, 100245.
30. A.G. Awale, S.B. Gholse and P.S. Utale, *Res. J. Chem. Sci*, **2013**, *3*, 81–87.
31. P.S. Yadav, D. Devprakash and G.P. Senthilkumar, **2011**, *3*, 1–7.
32. Y.J. Sahar, H. Mohammed and Z.N. Al-Abady, *Results Chem.*, **2023**, *5*, 100847.
33. H. Mohammed, *The Scientific World Journal*, **2021**, *2021*, 9943763.
34. M. hamady Manulla and A.K. Abbas, *Ibn AL-Haitham Journal For Pure and Applied Sciences*, **2025**, *38*, 266–277.
35. I.M. Shaker, H.A. Salih and S.M. Mahdi, *Int. J. ChemTech Res*, **2016**, *9*, 99–110.
36. J.M.M. Al-Zinke and A.J. Jarad, *J. Pharm. Sci. Res.*, **2019**, *11*, 98–103.
37. H.S. Mohammed, H.A. Al-Hasan, Z. Chaieb, Z. Zizi and H.N. Abed, *Bull. Chem. Soc. Ethiop.*, **2023**, *37*, 347–356.
38. S.S. Noor and I.K. Kareem, *Indones. J. Chem.*, **2024**, *24*, 822–834.